Chromosomal aberrations in PARP$^{-/-}$ mice: Genome stabilization in immortalized cells by reintroduction of poly(ADP-ribose) polymerase cDNA

Cynthia M. Simbulan-Rosenthal*†, Bassem R. Haddad†‡, Dean S. Rosenthal*†, Zoë Weaver§, Allen Coleman§, RuiBai Luo*, Hannah M. Young‡, Zhao-Qi Wang¶, Thomas Ried§, and Mark E. Smulson*‖

*Department of Biochemistry and Molecular Biology and the ‡Institute for Molecular and Human Genetics and Departments of Oncology and Obstetrics and Gynecology, Georgetown University School of Medicine, 3900 Reservoir Road NW, Washington, DC 20007; §National Cancer Institute, National Institutes of Health, Bethesda, MD 20892; and ¶International Agency for Research on Cancer, 69372 Lyon, France

Edited by Solomon H. Snyder, Johns Hopkins University School of Medicine, Baltimore, MD, and approved September 22, 1999 (received for review July 13, 1999)

Depletion of poly(ADP-ribose) polymerase (PARP) increases the frequency of recombination, gene amplification, sister chromatid exchanges, and micronuclei formation in cells exposed to genotoxic agents, implicating PARP in the maintenance of genomic stability. Flow cytometric analysis now has revealed an unstable tetraploid population in immortalized fibroblasts derived from PARP$^{-/-}$ mice. Comparative genomic hybridization detected partial chromosomal gains in 4C5-ter, 5F-ter, and 14A1-C1 in PARP$^{-/-}$mice and immortalized PARP$^{-/-}$fibroblasts. Neither the chromosomal gains nor the tetraploid population were apparent in PARP$^{-/-}$ cells stably transfected with PARP cDNA [PARP$^{-/-}$(+PARP)], indicating negative selection of cells with these genetic aberrations after reintroduction of PARP cDNA. Although the tumor suppressor p53 was not detectable in PARP$^{-/-}$ cells, p53 expression was partially restored in PARP$^{-/-}$(+PARP) cells. Loss of 14D3-ter that encompasses the tumor suppressor gene *Rb-1* in PARP$^{-/-}$ mice was associated with a reduction in retinoblastoma(Rb) expression; increased expression of the oncogene *Jun* was correlated with a gain in 4C5-ter that harbors this oncogene. These results further implicate PARP in the maintenance of genomic stability and suggest that altered expression of p53, Rb, and Jun, as well as undoubtedly many other proteins may be a result of genomic instability associated with PARP deficiency.

Poly(ADP-ribose) polymerase (PARP) is involved in nuclear processes involving cleavage and rejoining of DNA, such as DNA replication, differentiation, DNA repair and recombination, apoptosis, as well as maintenance of genomic stability (1, 2). Inhibition of PARP by either chemical inhibitors (3–5) or by dominant negative mutants (6, 7), or PARP depletion by antisense RNA expression (8, 9), results in an increased frequency of DNA strand breaks, recombination, gene amplification, micronuclei formation, and sister chromatid exchanges (SCE), all of which are markers of genomic instability, in cells exposed to DNA-damaging agents. PARP-deficient cell lines are hypersensitive to carcinogenic agents and also display increased SCE, implicating PARP as a guardian of the genome that facilitates DNA repair and protects against DNA recombination (10). We originally mapped the *PARP* gene to chromosome 1q41-q42 and *PARP*-like sequences to chromosomes 14q13-q32 and 13q34 (11); the latter pseudogene interrupts a *pol*-like element (12) and exhibits two-allele polymorphism (13) associated with predisposition to several cancers (14). Amplification of 1q41-q44 and increased PARP RNA expression are correlated with low genetic instability in human breast carcinomas (15).

PARP$^{-/-}$mice with a disrupted *PARP* gene do not express any immunodetectable PARP (16, 17). Although a novel activity capable of synthesizing poly(ADP-ribose) (PAR) recently has been shown in PARP$^{-/-}$ mice and cells derived from them, this residual activity, which is induced by DNA strand breaks, is only 5–10% of that in wild-type cells and has not been shown to modify proteins aside from itself, thus, it may not fully compensate for PARP depletion (18, 19). These mice are resistant to murine models of a number of human diseases, including focal cerebral ischemia (20), toxin-induced diabetes (21), 1-methyl-4-phenyl-1,2,3,6-tetrahydropyridine (MPTP)-induced Parkinsonism (22), and peroxynitrite-induced arthritis (23), suggesting that PARP activation, triggered by oxidative or nitrosative stress, plays a role in the pathophysiology of these diseases. Primary fibroblasts derived from PARP$^{-/-}$ mice show an elevated frequency of SCE and micronuclei in response to treatment with genotoxic agents (16, 24), further implicating PARP in the maintenance of genomic integrity. PARP$^{-/-}$ mice developed by another group exhibit extreme sensitivity to γ-irradiation and methylnitrosourea and increased genomic instability as revealed by a high level of SCE (17). Immortalized cells derived from these mice show retarded cell growth, G_2/M block, and chromosomal instability on exposure to DNA-alkylating agents, presumably because of a defect in DNA repair (25).

In the present study, flow cytometry revealed that immortalized fibroblasts derived from PARP$^{-/-}$ mice exhibit mixed ploidy, including a tetraploid cell population, which is also indicative of genomic instability. We characterized the genetic alterations associated with PARP depletion by comparative genomic hybridization (CGH) analysis (26, 27) of genomic DNA from both wild-type and PARP$^{-/-}$ mice as well as from immortalized fibroblasts derived from these animals. With a limit of detection of 5–10 Mb (28), this cytogenetic technique detects unbalanced chromosomal gains and losses in test DNA as a measure of genetic instability. Although CGH now is widely used as a powerful tool for generating maps of DNA copy number changes in human tumor genomes, only two studies to date have demonstrated its potential for evaluating genetic instability in transgenic mouse models (29, 30). CGH analysis revealed partial gains in chromosomes 4, 5, and 14, and partial loss of chromosome 14 in PARP$^{-/-}$ mice or immortalized PARP$^{-/-}$ fibroblasts. We further investigated the effect of stable transfection of PARP$^{-/-}$ cells with PARP cDNA on the genetic instability of these cells. Reintroduction of PARP cDNA into PARP$^{-/-}$ cells appeared to confer stability because the chromosomal gains as well as the unstable tetraploid population were no longer detected in these cells, further supporting an essential role for PARP in the maintenance of genomic stability.

This paper was submitted directly (Track II) to the PNAS office.

Abbreviations: PAR, poly(ADP-ribose); PARP, poly(ADP-ribose) polymerase; SCE, sister chromatid exchanges; CGH, comparative genomic hybridization; PCNA, proliferating cell nuclear antigen; topo I, topoisomerase I; RT-PCR, reverse transcription–PCR; Rb, retinoblastoma.

†C.M.S.-R., B.R.H., and D.S.R. contributed equally to this work.

‖To whom reprint requests should be addressed at: Department of Biochemistry and Molecular Biology, Georgetown University School of Medicine, 3900 Reservoir Road NW, Washington, DC 20007. E-mail: smulson@bc.georgetown.edu.

The publication costs of this article were defrayed in part by page charge payment. This article must therefore be hereby marked "*advertisement*" in accordance with 18 U.S.C. §1734 solely to indicate this fact.

Materials and Methods

Cell Lines, Vectors, and Transfection. Homozygous PARP$^{-/-}$ mice that were generated by disrupting exon 2 of the *PARP* gene by homologous recombination (16) and wild-type (PARP$^{+/+}$) littermates (strain 129/Sv × C57BL/6; female) were used in the present study. Wild-type (PARP$^{+/+}$ clone A19) and PARP$^{-/-}$ (clone A1) fibroblasts were immortalized spontaneously by a standard 3T3 protocol (16) and cultured in DMEM supplemented with 10% FBS, penicillin (100 units/ml), and streptomycin (100 μg/ml). Immortalized PARP$^{-/-}$ fibroblasts were cotransfected by Lipofectamine (Life Technologies, Grand Island, NY) with human PARP (pCD12) cDNA (31) and the plasmid pTracer-CMV (a zeocin-based vector system; Invitrogen). This vector was used because the PARP$^{-/-}$ fibroblasts express a neomycin resistance gene that was introduced during establishment of the PARP knockout mice. Stable transfectants were selected in growth medium containing zeocin (500 μg/ml).

Immunoblot Analysis. SDS/PAGE and transfer of proteins to nitrocelluose membranes were performed according to standard procedures. Membranes were stained with Ponceau S (0.5%) to confirm equal loading and transfer of proteins. Membranes were incubated with antibodies to PARP (1:2,000 dilution; BioMol, Plymouth Meeting, PA), PAR (1:250; gift from M. Miwa, Japan), p53 (1:20 dilution; PAb421, Calbiochem), retinoblastoma (Rb) (1:200 dilution; clone IF8, Santa Cruz Biotechnology), glutamate dehydrogenase (1:1,000; Biodesign International, Kennebunkport, ME), Jun (1:1,000 dilution, Calbiochem), proliferating cell nuclear antigen (PCNA) (1:800; Calbiochem), or topoisomerase I (topo I) (1:2,500; TopoGen, Columbus, OH). After subsequent incubation with appropriate horseradish peroxidase-conjugated antibodies to mouse or rabbit IgG (1:3,000 dilution), immune complexes were detected by enhanced chemiluminescence (Pierce).

Flow Cytometry. Nuclei were prepared for flow cytometric analysis as described (33). Cells were exposed to trypsin and resuspended in 100 μl of a solution containing 250 mM sucrose, 40 mM sodium citrate (pH 7.6), and 5% (vol/vol) DMSO. The cells were lysed for 10 min in a solution containing 3.4 mM sodium citrate, 0.1% (vol/vol) NP-40, 1.5 mM spermine tetrahydrochloride, and 0.5 mM Tris·HCl (pH 7.6). After incubation of lysates for 10 min with ribonuclease A (0.1 mg/ml), nuclei were stained for 15 min with propidium iodide (0.42 mg/ml), filtered through a 37-μm nylon mesh, and analyzed with a dual-laser flow cytometer (FACScan, Becton Dickinson).

CGH. Normal DNA was extracted from spleen tissue of normal mice (FVB) and test DNA was prepared from liver tissue of wild-type and PARP$^{-/-}$ mice, as well as from immortalized PARP$^{-/-}$ and PARP$^{-/-}$(+PARP) fibroblasts according to standard protocols. Differences in the source of the DNA (spleen, liver, or cell lines) does not affect CGH results (26, 27). Normal metaphase chromosomes for CGH were prepared from a spleen culture of C57BL/6 mice as described (30). Labeling, hybridization, and detection of DNA were performed as described (30, 34). Normal DNA and test DNA were labeled in a nick-translation reaction in which dTTP was replaced by digoxigenin-11-dUTP (Boehringer Mannheim) (normal DNA) or biotin-16-dUTP (Boehringer Mannheim) (test DNA). A total of 500 ng each of labeled normal and test DNA was precipitated with ethanol in the presence of salmon sperm DNA (3 μg) and excess mouse Cot-1 DNA (50 μg) (GIBCO/BRL), and the precipitates were dried and resuspended in 15 μl of hybridization solution (50% formamide, 2× SSC, 10% dextran sulfate). The DNA was denatured at 80°C for 10 min and allowed to preanneal for 3 h at 37°C. Normal metaphase chromosomes were denatured at 80°C for 2 min in 2× SSC containing 70% formamide and then were dehydrated through an ethanol series (70%, 90%, and 100%). The probe mixture was applied to the denatured metaphase chromosomes under a coverslip and sealed with rubber cement, and hybridization was performed for 4 days at 37°C. The biotin-labeled test DNA was visualized with FITC-conjugated avidin (Vector Laboratories), and the digoxigenin-labeled control DNA was detected with mouse anti-digoxigenin (Sigma) and tetramethylrhodamine isothiocyanate-conjugated goat antibodies to mouse IgG (Sigma). Chromosomes were counterstained with 4′,6-diamidino-2-phenylindole (DAPI) and embedded in antifading agent.

Microscopy and Digital Image Analysis. Gray scale images of FITC-labeled test DNA, the tetramethylrhodamine isothiocyanate-labeled control DNA, and the 4′,6-diamidino-2-phenylindole (DAPI) counterstain from at least eight metaphase spreads for each hybridization were acquired with a cooled charge-coupled device camera (CH250; Photometrics, Tucson, AZ) that was connected to a Leica DMRBE microscope equipped with fluorochrome-specific optical filters TR1, TR2, and TR3 (Chroma Technology, Brattleboro, VT). Quantitative evaluation of hybridization was performed with a custom computer program developed for analysis of mouse chromosomes that was based on a human CGH program (30, 35). Average ratio profiles were computed as the mean value of at least eight ratio images. Fluorescence ratio is defined as the ratio of the total test (green) to the total control (red) fluorescence at each position along the length of each chromosome; chromosomal regions with a fluorescence ratio of ≥ 1.25 were interpreted as a gain, whereas regions with a ratio of ≤ 0.75 were interpreted as a loss.

PCR and Reverse Transcription-PCR (RT-PCR). Unique oligonucleotide primer pairs for human and mouse *PARP*, *p53*, and *Rb-1* genes and mRNA were designed and prepared. Total RNA, purified from cell pellets or liver tissue with an RNA extraction kit (Amersham Pharmacia Biotech), was subjected to RT-PCR with a Perkin–Elmer Gene Amp EZ rtTh RNA PCR kit. The reaction mix (50 μl) contained 300 μM each of dGTP, dATP, dTTP, and dCTP, 0.45 μM of each primer, 1 μg of total RNA, and rTth DNA polymerase (5 units). With an Amplitron II PCR machine (Thermolyne, Dubuque, IA), RNA was transcribed at 65°C for 40 min, and DNA was amplified by an initial incubation at 95°C for 2 min, followed by 40 cycles of 95°C for 1 min, 60°C for 1.5 min, and 65°C for 0.5 min, and a final extension at 70°C for 22 min. For PCR, genomic DNA was prepared according to standard protocols and amplified as above. The PCR products then were separated by electrophoresis in a 1.5% agarose gel and visualized by ethidium bromide staining.

Results

An Unstable Tetraploid Population in Immortalized PARP$^{-/-}$ Cells. One marker of genomic instability in cells is the development of tetraploidy or aneuploidy, which is typical of many tumors and is associated with progression to malignancy or metastasis (36). Tetraploidy results when cells exit from mitosis in the absence of either chromosome segregation or cytokinesis; such cells are genetically unstable and become aneuploid at subsequent mitoses (37). Flow cytometric analysis of immortalized fibroblasts derived from PARP knockout mice (clone A1) revealed the existence of a tetraploid population of cells (Fig. 1). After cell synchronization and release from either aphidicolin block at the G_1-S transition or serum deprivation, DNA histograms of wild-type cells (clone A19) (Fig. 1*A*) showed a typical pattern characterized by two major peaks of nuclei at G_0-G_1 (haploid) and G_2-M (diploid) phases of the cell cycle. In contrast, in addition to these two major peaks, DNA histograms of PARP$^{-/-}$ cells (clone A1) (Fig. 1*B*) showed a third peak corresponding to the G_2-M peak of an unstable tetraploid cell population in these cells. Similar to those of wild-type cells, DNA histograms of PARP$^{-/-}$ cells stably transfected with PARP cDNA [PARP$^{-/-}$(+PARP)] (clone A3–2) and synchronized by serum deprivation exhibited only the two major peaks of nuclei at

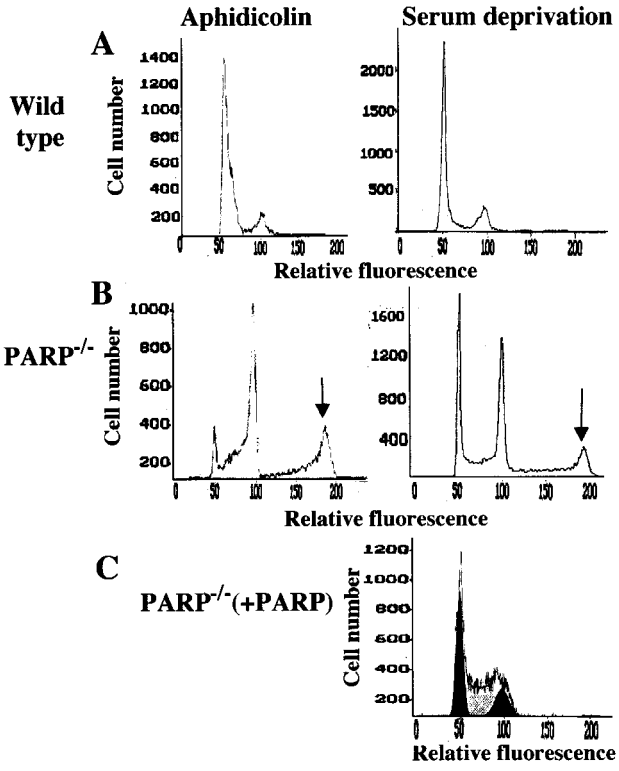

Fig. 1. Flow cytometric analysis of immortalized wild-type (*A*), PARP$^{-/-}$ (*B*), and PARP$^{-/-}$(+PARP) (*C*) fibroblasts. Cells were harvested 5 h after release from aphidicolin-induced G_1-S block (*Left*) or 18 h after release from serum deprivation (*Right*). Nuclei then were prepared and stained with propidium iodide for flow cytometric analysis. In addition to the two major peaks of nuclei at G_0-G_1 and G_2-M apparent in the DNA histograms of wild-type and PARP$^{-/-}$(+PARP) cells, the DNA histograms of PARP$^{-/-}$ cells exhibit a third peak corresponding to the G_2-M peak of an unstable tetraploid cell population (arrows).

G_0-G_1 and G_2-M (Fig. 1*C*). Thus, stable transfection of PARP$^{-/-}$ cells with PARP cDNA appeared to confer genomic stability to the PARP$^{-/-}$(+PARP) cells. Loss of PARP may allow the emergence and survival of cells with gross genetic abnormalities that normally would have been repaired.

Lack of p53 Protein Caused by PARP Deficiency in Immortalized PARP$^{-/-}$ Cells; Partial Restoration of p53 Expression by Reintroduction of PARP cDNA. Inactivation or loss of the tumor suppressor protein p53 in diploid cells results in the formation of unstable tetraploid cells predisposed to chromosome segregation abnormalities (38). We therefore investigated whether development of the unstable population of tetraploid cells in immortalized PARP$^{-/-}$ fibroblasts might be associated with loss of p53 expression. Immunoblot analysis with antibodies to PARP confirmed the lack of immunoreactive PARP in immortalized PARP$^{-/-}$ cells and its presence in wild-type and PARP$^{-/-}$(+PARP) cells (Fig. 2*A*). PARP$^{-/-}$(+PARP) cells were stably transfected with human PARP cDNA; thus, RT-PCR analysis detected mouse or human PARP transcripts in wild-type and PARP$^{-/-}$(+PARP) cells, respectively, but not in PARP$^{-/-}$cells. Reconstitution of PARP activity in PARP$^{-/-}$(+PARP) cells was further verified by immunoblot analysis with antibodies to PAR. PARP expression also was confirmed in tissue extracts of wild-type, but not PARP$^{-/-}$, mice, by immunoblot analysis with anti-PARP; reprobing of the blot with anti-PAR revealed negligible poly(ADP-ribosyl)ation of nuclear proteins in PARP$^{-/-}$ tissue extracts (data not shown).

p53 was detected in lysates of wild-type cells, but not in PARP$^{-/-}$ cell extracts, by immunoblot analysis with antibodies to p53

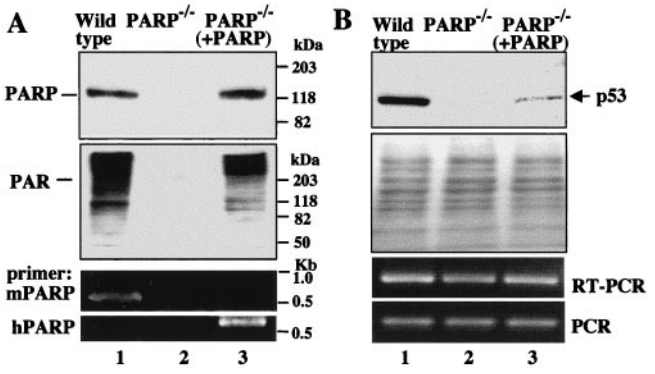

Fig. 2. PARP and p53 expression in immortalized wild-type, PARP$^{-/-}$, and PARP$^{-/-}$(+PARP) fibroblasts. (*A*) Cell extracts of wild-type, PARP$^{-/-}$, and PARP$^{-/-}$(+PARP) fibroblasts (30 μg protein) were subjected to immunoblot analysis with antibodies to PARP (*Top*) and to PAR (*Middle*). RT-PCR was performed with specific human (hPARP) and mouse (mPARP) PARP primers (*Bottom*). (*B*) Cell extracts were subjected to immunoblot analysis with mAb to p53 (PAb421) (*Top*). The blot was stained with Ponceau S to verify equal loading and transfer of proteins in both lanes (*Middle*). RT-PCR and PCR were performed with specific primers for p53 mRNA and gene (*Bottom*). The positions of PARP, PAR, p53, and PARP and p53 cDNA are indicated.

(PAb421) (Fig. 2*B*). Stable transfection with PARP cDNA partially restored p53 expression in the PARP$^{-/-}$(+PARP) cells. Consistent with other studies (39), the decrease in p53 expression in PARP$^{-/-}$ cells was not attributable to lower p53 transcript levels or a decrease in copy number, as revealed by RT-PCR analysis of RNA and PCR analysis of genomic DNA from these cells. This finding suggests that the lack of p53 in PARP$^{-/-}$ cells may be the result of reduced protein stability and that PARP may be involved in p53 stabilization and accumulation. Because the loss of p53 allows the survival of cells with severe DNA damage, thus, promoting tetraploidy (40), down-regulation of p53 expression in PARP$^{-/-}$ cells may contribute, at least in part, to the genomic instability and the development of tetraploidy in these cells.

CGH Analysis of Chromosomal Aberrations Associated with PARP Deficiency. CGH was used in the present study to map chromosomal gains and losses associated with PARP depletion. CGH analysis of DNA from liver tissue of PARP$^{-/-}$ mice revealed partial gains in chromosome 4 (4C5-ter), chromosome 5 (5F-ter), and chromosome 14 (14A1-C2), as well as a deletion that mapped to chromosome 14 (14D3-ter) (Fig. 3*B*). In contrast, CGH analysis detected no chromosomal abnormalities in wild-type (PARP$^{+/+}$) mice (Fig. 3*A*). These results indicate that the specific chromosomal changes detected in the PARP$^{-/-}$ mice are attributable to PARP deficiency.

To investigate the effects of reintroduction of PARP cDNA into PARP$^{-/-}$ cells, CGH analysis also was performed on genomic DNA from immortalized PARP$^{-/-}$ (clone A1) and PARP$^{-/-}$(+PARP) (clone A3–2) fibroblasts that had been passaged for >10 generations. The partial chromosomal gains detected at 4C5-ter, 5F-ter, and 14A1-C2 in PARP$^{-/-}$ mice were also present in the immortalized PARP$^{-/-}$ fibroblasts (Fig. 4*B*). However, these gains were not detected in the average ratio profiles of genomic DNA from PARP$^{-/-}$(+PARP) cells (Fig. 4*C*). Only the partial loss of chromosome 14 was retained in these cells. Additional chromosomal aberrations were detected by CGH in both the immortalized PARP$^{-/-}$ and PARP$^{-/-}$(+PARP) cells, which are likely attributable to the immortalization process (data not shown).

Altered Expression of Tumor Suppressor *Rb-1* and the *Jun* Oncogene in PARP$^{-/-}$ Mice. Deletions or gains of chromosomal regions detected by CGH may indicate the site of genes that promote further genomic instability through loss of tumor suppressor

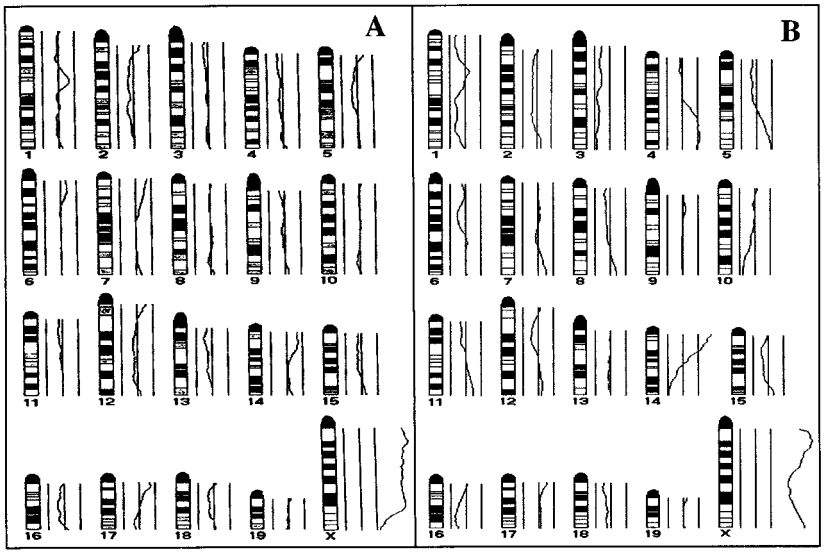

Fig. 3. CGH average ratio profiles of genomic DNA from liver tissue of wild-type (*A*) and PARP$^{-/-}$ (*B*) mice. Average ratio profiles were computed for all chromosomes and used for the mapping of changes in copy number. The three vertical lines to the right of the chromosome ideograms represent values of 0.75, 1, and 1.25 (left to right, respectively) for the fluorescence ratio between the test DNA and the normal control DNA. The ratio profile (curve) was computed as a mean value of at least eight metaphase spreads. A ratio of $\geq$ 1.25 was regarded as a gain and a ratio of $\leq$ 0.75 as a loss.

genes or gains of oncogenes. It was therefore of interest to assess the expression of some key genes that map to regions of chromosomal gain or loss in the PARP$^{-/-}$ mice, although clearly many other genes could have been chosen. The region of chromosome 14 that is deleted in PARP$^{-/-}$ mice (14D3-ter) encompasses the tumor suppressor gene *Rb-1* (Fig. 5*A*) along with numerous other genes. Interestingly, immunoblot analysis of tissue extracts with antibodies to Rb revealed a marked reduction in constitutive expression of Rb in PARP$^{-/-}$ mice relative to that in wild-type mice. Rb expression also was decreased in immortalized PARP$^{-/-}$ fibroblasts compared with wild-type fibroblasts (data not shown). Similarly, the glutamate dehydrogenase (*Glud*) gene, a neighboring gene that also maps to 14D3, exhibits reduced expression in the PARP$^{-/-}$ mice as shown by lower levels of the glutamate dehydrogenase protein in tissue extracts. In addition, the oncogene *Jun* is located (at 4C5-C7) in the region of chromosome 4 that exhibits a gain in PARP$^{-/-}$ mice and cells. Immunoblot analysis of tissue extracts with antibodies to Jun confirmed that Jun expression is increased in PARP$^{-/-}$ mice (Fig. 5*B*). In contrast, no difference in protein expression of the *Pcna* and *Top1* genes was detected in wild-type and PARP$^{-/-}$ mice (Fig. 5*C*); these genes map to chromosome 2B-C and 2H, respectively, regions that show no gains or losses by CGH analysis.

A marked decrease in Rb transcript levels in PARP$^{-/-}$ mice, as revealed by RT-PCR analysis, correlates with decreased abundance of Rb protein in these animals (Fig. 5*D*). In contrast, p53 transcript levels were similar in wild-type and PARP$^{-/-}$ mice, in agreement with CGH results showing that the *Rb* gene, but not the *p53* gene (located in chromosome 11B2-C), is in a deleted chromosomal region. PCR analysis of DNA from liver tissue further revealed that the Rb gene copy number also is reduced in PARP$^{-/-}$ mice compared with wild-type mice, whereas the p53 gene copy number is unchanged (Fig. 5*D*). Thus, the decreases in Rb protein and transcript levels in PARP$^{-/-}$ mice are consistent with the loss of the *Rb* gene.

Discussion

Although exhibiting varying phenotypes, two groups of PARP knockout mice developed by different laboratories both exhibit increased genomic instability as indicated by elevated frequencies of SCE and micronuclei formation after treatment with DNA-damaging agents, providing support for a role for PARP in the maintenance of genomic integrity (16, 17). We have now identified a population of tetraploid cells, another indication of genetic instability (37), among immortalized fibroblasts derived from PARP$^{-/-}$ mice. This tetraploid cell population was no longer apparent in PARP$^{-/-}$(+PARP) cells, suggesting that the reintroduction of PARP into PARP$^{-/-}$ cells may have stabilized the genome and resulted in selection against this genomically unstable population.

CGH analysis revealed that PARP knockout mice and immortalized fibroblasts derived from these animals exhibit similar chromosomal aberrations, including gains in regions of chromosomes 4, 5, and 14. In contrast, the CGH profile of DNA from wild-type (PARP$^{+/+}$) mice showed no DNA gains or losses, indicating that the chromosomal imbalances detected in the PARP$^{-/-}$ genome are caused by PARP deficiency. Interestingly, the chromosomal gains in the PARP$^{-/-}$ genome were no longer detected in the CGH profiles of DNA from PARP$^{-/-}$(+PARP)

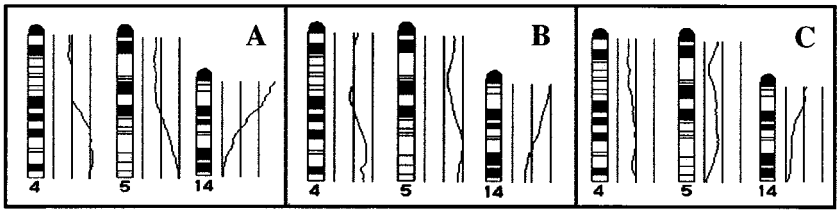

Fig. 4. Comparison of the CGH profiles of chromosomes 4, 5, and 14 among PARP$^{-/-}$ mice (*A*) and immortalized PARP$^{-/-}$ (*B*) and PARP$^{-/-}$(+PARP) (*C*) fibroblasts. Average ratio profiles were computed for all chromosomes from at least eight metaphase spreads as described in Fig. 3, with only the results for chromosomes 4, 5, and 14 shown. PARP$^{-/-}$(+PARP) fibroblasts did not show the gains at 4C5-ter, 5F-ter, or 14A1-C2 that were apparent in both PARP$^{-/-}$ mice and immortalized PARP$^{-/-}$ cells, although they retained the partial loss at 14D3-ter.

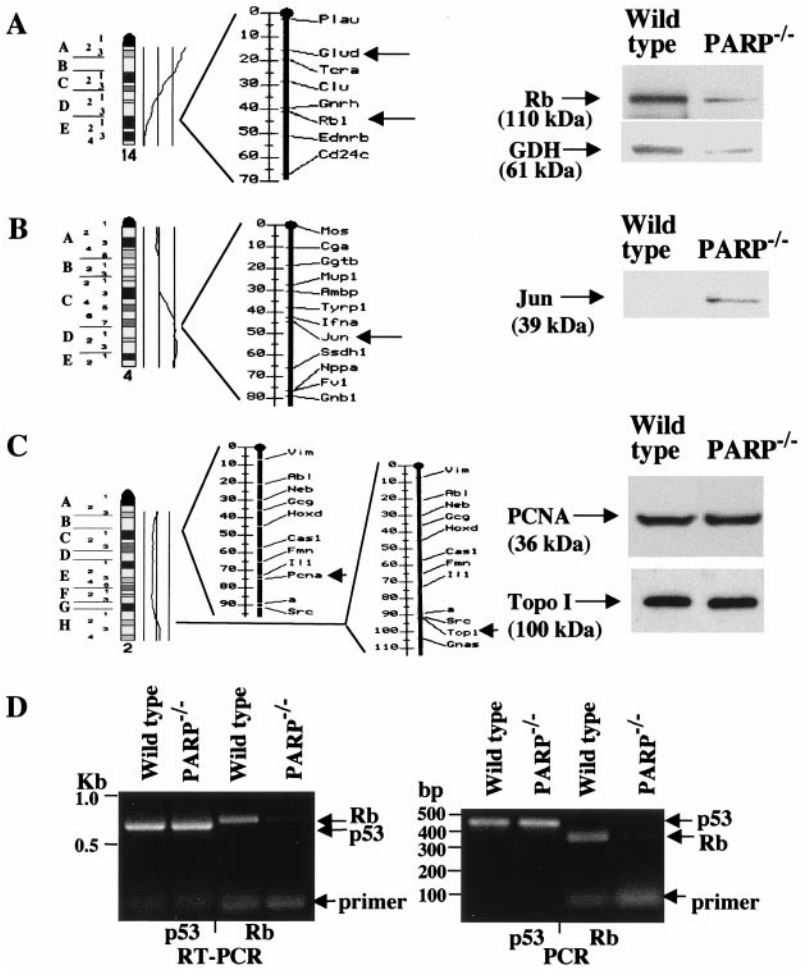

Fig. 5. Location of *Rb-1* and *Jun* in chromosomal regions with copy number changes in PARP$^{-/-}$ mice and altered expression of Rb and Jun in these animals. (*A*) CGH profile of chromosome 14 of the PARP$^{-/-}$ mice showing the loss of 14D3-ter, and the location of *Rb-1* and *Glud* (arrows) on 14D3. Immunoblot analysis with antibodies to Rb and glutamate dehydrogenase (GDH) of tissue extracts from wild-type and PARP$^{-/-}$ mice. (*B*) CGH profile of chromosome 4 of PARP$^{-/-}$ mice showing the partial gain of 4C5-ter and the location of *Jun* (arrow) on mouse chromosome 4C5. The immunoblot in *A* was reprobed with antibodies to Jun. (*C*) Balanced CGH profile of chromosome 2 of PARP$^{-/-}$ mice and the location of *Pcna* and *Topl* genes (arrows) on 2B-C and 2H. The immunoblot in *A* was reprobed with antibodies to PCNA and to topo I. The positions of Rb (110 kDa), glutamate dehydrogenase (61 kDa), Jun (39 kDa), PCNA (36 kDa), and topo I (100 kDa) are indicated. (*D*) RT-PCR and PCR analysis of wild-type and PARP$^{-/-}$ mice liver using p53 and Rb-specific primers. The positions of p53 and Rb cDNA (arrows) and of DNA size standards (in kb and bp) are indicated.

cells. The loss of 14D3-ter that encompasses the tumor suppressor gene *Rb-1* and presumably numerous other genes from the genome of PARP$^{-/-}$ mice was associated with a marked reduction in Rb protein, transcript, and gene copy number in these animals. Furthermore, increased expression of the oncogene *Jun* in the PARP$^{-/-}$ mice also was correlated with a gain in 4C5-ter that harbors the *Jun* oncogene. In contrast, there was no difference in expression of the *Pcna* and *Top1* genes in wild-type and PARP$^{-/-}$ mice; these genes are considered unaffected by location within a region of chromosomal gain or loss. These results suggest that the gain or loss of large chromosomal regions, such as that encompassing *Rb-1* and numerous other genes, is caused by PARP deletion and concomitant genomic instability in the PARP$^{-/-}$ mice.

The loss of tetraploidy and the chromosomal gains in the PARP$^{-/-}$ cells after stable transfection of PARP cDNA provide further support for an apparent essential role of PARP in the maintenance of genomic stability. One mechanism by which PARP may confer genetic stability is via its putative role in p53 induction, accumulation, and stabilization. p53 is involved in the maintenance of diploidy as a component of the spindle checkpoint (41) and by regulating centrosome duplication (42). Given that the loss of p53 from diploid cells promotes the survival of cells with severe DNA damage and the development of tetraploidy (38, 40, 41), the presence of a tetraploid population among the immortalized PARP$^{-/-}$ cells is consistent with the lack of immunoreactive p53 in these cells. Cells that are incapable of poly(ADP-ribosyl)ation because of unavailability of NAD (43) and primary fibroblasts from PARP$^{-/-}$ mice (44) also show reduced basal levels of p53 and defective p53 induction in response to DNA damage. Interestingly, the loss of the tetraploid population in the PARP$^{-/-}$(+PARP) cells further correlates with the partial restoration of p53 expression in these cells.

We recently showed that p53 is extensively poly(ADP-ribosyl)ated by PARP during early apoptosis and that degradation of the PAR attached to p53 coincides with expression of p53-responsive genes, suggesting that poly(ADP-ribosyl)ation may regulate p53-mediated transcriptional activation of these genes (45). The location of a PAR attachment site adjacent to a proteolytic cleavage site in p53 further suggests that PAR may protect p53 from proteolysis (46); similar protection has been noted after binding of mAbs adjacent to this region (47). The lack of regularly spliced wild-type p53 in PARP$^{-/-}$ cells also has been attributed to decreased protein stability, not lower levels of p53 mRNA (39). Consistently, RT-PCR and PCR analysis of RNA and DNA from immortalized wild-type and PARP$^{-/-}$cells revealed that reduced expression of p53 in the PARP$^{-/-}$ cells was not attributable to lower levels of p53 transcripts or a decrease in p53 gene copy number. Modification of p53 by PARP therefore is implicated in p53 accumulation and stabilization (45, 46, 48), which may explain the apparent lack of p53 in PARP$^{-/-}$ cells. Lack of p53 in PARP$^{-/-}$ cells may promote further genomic alterations via different mechanisms, including abnormal centrosome amplification, which is associated with lack of wild-type p53 and also generates numerical chromosome aberrations (49).

p53 monitors genomic integrity and reduces the occurrence of mutations either by mediating cell cycle arrest in G_1 or at G_2-M or by inducing apoptosis in cells that have accumulated substantial DNA damage (50, 51). Increased expression of the p53 homolog

p73 may compensate for the lack of wild-type p53 in immortalized PARP$^{-/-}$ cells (39). Consistently, the region of chromosome 4 (4C5-ter) that shows a gain in PARP$^{-/-}$mice harbors the *p73* gene. However, although p73, when overexpressed, can activate p53-responsive genes and induce apoptosis, it is unable to detect DNA lesions and, thus, is not induced by DNA damage (52). Both PARP activity and p53 accumulation are induced by DNA damage, and both proteins have been implicated as sensors of such damage. A functional association of PARP and p53 has been suggested by immunoprecipitation experiments (53). PARP cycles on and off the ends of DNA in the presence of NAD, and its automodification during DNA repair *in vitro* facilitates access to DNA repair enzymes (54, 55). Thus, both the increased sensitivity of PARP$^{-/-}$ mice and cells to DNA-damaging agents (17, 25) and their genetic instability are consistent with their deficiencies in PARP and p53. Our results suggest that some of the consequences of PARP deficiency in PARP$^{-/-}$ mice may be attributed, at least in part, to indirect effects resulting from changes in other DNA damage checkpoint proteins, such as p53.

We also have shown that, whereas immortalized wild-type fibroblasts exhibit an early activation of PARP and a rapid Fas-mediated apoptotic response, PARP$^{-/-}$ cells do not; stable transfection of PARP$^{-/-}$ cells with PARP cDNA renders the cells sensitive to Fas-mediated apoptosis, indicating a role for PARP and poly(ADP-ribosyl)ation in the early stages of this death program (32). Immortalized PARP$^{-/-}$ cells also show severe defects in base-excision DNA repair, as indicated by a delay in rejoining of DNA strand breaks after exposure to genotoxic agents (25). It is therefore conceivable that the loss of PARP and the lack of p53 expression in PARP$^{-/-}$ cells may allow the survival of cells with gross genetic abnormalities because of both an impaired ability to perform efficient DNA repair (25) and to undergo Fas-mediated apoptosis (32) in cells that have accumulated substantial DNA damage.

This work was supported in part by Grants CA25344 and 1P01 CA74175 from the National Cancer Institute, by the United States Air Force Office of Scientific Research (Grant AFOSR-89–0053), and by the United States Army Medical Research and Development Command (Contract DAMD17–90-C-0053 to M.E.S. and DAMD 17–96-C-6065 to D.S.R).

1. Althaus, F. R., Hilz, H. & Shall, S. (1985) *ADP-Ribosylation of Proteins* (Springer, Berlin).
2. Jacobson, M. K. & Jacobson, E. L. (1989) *ADP-Ribose Transfer Reactions: Mechanisms and Biological Significance* (Springer, New York).
3. Morgan, W. & Cleaver, J. (1982) *Mutat. Res.* **104,** 361–366.
4. Burkle, A., Heilbronn, R. & Zur, H. H. (1990) *Cancer Res.* **50,** 5756–5760.
5. Waldman, A. & Waldman, B. (1991) *Nucleic Acids Res.* **19,** 5943–5947.
6. Schreiber, V., Hunting, D., Trucco, C., Gowans, B., Grunwald, P., de Murcia, G. & de Murcia, J. (1995) *Proc. Natl. Acad. Sci. USA* **92,** 4753–4757.
7. Kupper, J., Muller, M. & Burkle, A. (1996) *Cancer Res.* **56,** 2715–2717.
8. Ding, R., Pommier, Y., Kang, V. H. & Smulson, M. (1992) *J. Biol. Chem.* **267,** 12804–12812.
9. Ding, R. & Smulson, M. (1994) *Cancer Res.* **54,** 4627–4634.
10. Chatterjee, S., Berger, S. & Berger, N. (1999) *Mol. Cell. Biochem.* **193,** 23–30.
11. Cherney, B. W., McBride, O. W., Chen, D. F., Alkhatib, H., Bhatia, K., Hensley, P. & Smulson, M. E. (1987) *Proc. Natl. Acad. Sci. USA* **84,** 8370–8374.
12. Lyn, D., Deaven, L., Istock, N. & Smulson, M. (1993) *Genomics* **18,** 206–211.
13. Lyn, D., Cherney, B., Lalande, M., Berenson, J., Lupold, S., Bhatia, K. & Smulson, M. (1993) *Am. J. Hum. Genet.* **52,** 124–134.
14. Bhatia, K. G., Cherney, B. W., Huppi, K., Magrath, I. T., Cossman, J., Sausville, E., Barriga, F., Johnson, B., Gause, B., Bonney, G., *et al*. (1990) *Cancer Res.* **50,** 5406–5413.
15. Bieche, I., de Murcia, G. & Lidereau, R. (1996) *Clin. Cancer Res.* **2,** 1163–1167.
16. Wang, Z. Q., Auer, B., Stingl, L., Berghammer, H., Haidacher, D., Schweiger, M. & Wagner, E. F. (1995) *Genes Dev.* **9,** 509–520.
17. de Murcia, J., Niedergang, C., Trucco, C., Ricoul, M., Dutrillaux, B., Mark, M., Oliver, J., Masson, M., Dierich, A., LeMeur, M., *et al*. (1997) *Proc. Natl. Acad. Sci. USA* **94,** 7303–7307.
18. Shieh, W. M., Ame, J. C., Wilson, M., Wang, Z. Q., Koh, D., Jacobson, M. & Jacobson, E. (1998) *J. Biol. Chem.* **273,** 30069–30072.
19. Ame, J., Rolli, V., Schreiber, V., Niedergang, C., Apiou, F., Decker, P., Muller, S., Hoger, T., de Murcia, J. & de Murcia, G. (1999) *J. Biol. Chem.* **274,** 17860–17868.
20. Eliasson, M., Sampei, K., Mandir, A., Hurn, P., Traystman, R., Bao, J., Pieper, A., Wang, Z. Q., Dawson, T., Snyder, S. & Dawson, V. (1997) *Nat. Med.* **3,** 1089–1095.
21. Pieper, A., Brat, D., Krug, D., Watkin, C., Gupta, S., Blackshaw, S., Verma, A., Wang, Z. Q. & Snyder, S. (1999) *Proc. Natl. Acad. Sci. USA* **96,** 3059–3064.
22. Mandir, S., Przedboeski, S., Jackson-Lewis, V., Wang, Z. Q., Simbulan-Rosenthal, C., Smulson, M., Hoffman, B., Guastella, D., Dawson, V. & Dawson, T. (1999) *Proc. Natl. Acad. Sci. USA* **96,** 5774–5779.
23. Szabo, C., Virag, L., Cuzzocrea, S., Scott, G., Hake, P., O'Connor, M., Zingarelli, B., Salzman, A. & Kun, E. (1998) *Proc. Natl. Acad. Sci. USA* **95,** 3867–3872.
24. Wang, Z., Stingl, L., Morrison, C., Jantsch, M., Los, M., Schulze-Osthoff, K. & Wagner, E. (1997) *Genes Dev.* **11,** 2347–2358.
25. Trucco, C., Oliver, F., de Murcia, G. & de Murcia, J. (1998) *Nucleic Acids Res.* **26,** 2644–2649.
26. Kallioniemi, A., Kallioniemi, O.-P., Sudar, D., Rutovitz, D., Gray, J., Waldman, F. & Pinkel, D. (1992) *Science* **258,** 818–821.
27. Du Manoir, S., Speicher, M., Joos, S., Schrock, E., Popp, S., Dohner, H., Kovacs, G., Robert-Nicoud, M., Lichter, P. & Cremer, T. (1993) *Hum. Genet.* **90,** 590–610.
28. Forozan, F., Karhu, K., Kononen, J., Kallionemi, A. & Kallionemi, O. (1997) *Trends Genet.* **13,** 405–409.
29. Shi, Y., Naik, P., Dietrich, W., Gray, J., Hanahan, D. & Pinkel, D. (1997) *Genes Chromosomes Cancer* **2,** 104–111.
30. Weaver, Z., McCormack, S., Liyanage, M., du Manoir, S., Coleman, A., Schrock, E., Dickson, R. & Ried, T. (1999) *Genes Chromosomes Cancer* **25,** 251–260.
31. Alkhatib, H. M., Chen, D. F., Cherney, B., Bhatia, K., Notario, V., Giri, C., Stein, G., Slattery, E., Roeder, R. G. & Smulson, M. E. (1987) *Proc. Natl. Acad. Sci. USA* **84,** 1224–1228.
32. Simbulan-Rosenthal, C. M., Rosenthal, D. S., Iyer, S., Boulares, A. H. & Smulson, M. E. (1998) *J. Biol. Chem.* **273,** 13703–13712.
33. Vindelov, L. L., Christensen, I. J., Jensen, G. & Nissen, N. I. (1983) *Cytometry* **3,** 332–339.
34. Figueiredo, B., Stratakis, C., Sandrini, R., DeLacerda, L., Pianovsky, M., Young, H. & Haddad, B. (1999) *J. Clin. Endocrinol. Metab.* **84,** 1116–1121.
35. du Manoir, S., Schrock, E., Bentz, M., Speicher, M., Joos, M., Ried, T., Lichter, P. & Cremer, T. (1995) *Cytometry* **19,** 24–41.
36. Robinson, J., Rademaker, A., Goolsby, C., Traczyk, T. & Zoladz, C. (1996) *Cancer* **77,** 284–291.
37. Andreassen, P., Martineau, S. & Margolis, R. (1996) *Mutat. Res.* **372,** 181–194.
38. Ramel, S., Sanchez, C., Schimke, M., Neshat, K., Cross, S., Raskind, W. & Reid, B. (1995) *Pancreas* **11,** 213–222.
39. Schmid, G., Wang, Z. Q. & Wesierska-Gadek, J. (1999) *Biochem. Biophys. Res. Commun.* **255,** 399–405.
40. Yin, X., Grove, L., Datta, N., Long, M. & Prochownik, E. (1999) *Oncogene* **18,** 1177–1184.
41. Cross, S., Sanchez, C., Morgan, C., Schimke, M., Ramel, S., Idzerda, R., Raskind, W. & Reid, B. (1995) *Science* **267,** 1353–1356.
42. Fukasawa, K., Choi, T., Kuriyama, R., Rulong, S. & Vande Woude, G. (1996) *Science* **271,** 1744–1747.
43. Whitacre, C. M., Hashimoto, H., Tsai, M.-L., Chatterjee, S., Berger, S. J. & Berger, N. A. (1995) *Cancer Res.* **55,** 3697–3701.
44. Agarwal, M., Agarwal, A., Taylor, W., Wang, Z. Q. & Wagner, E. (1997) *Oncogene* **15,** 1035–1041.
45. Simbulan-Rosenthal, C. M., Rosenthal, D. S. & Smulson, M. E. (1999) *Cancer Res.* **59,** 2190–2194.
46. Malanga, M., Pleschke, J., Kleczkowska, H. & Althaus, F. (1998) *J. Biol. Chem.* **273,** 11839–11843.
47. Li, X. & Coffino, P. (1996) *J. Biol. Chem.* **271,** 4447–4451.
48. Simbulan-Rosenthal, C. M., Rosenthal, D. S., Ding, R., Bhatia, K. & Smulson, M. E. (1998) *Biochem. Biophys. Res. Commun.* **253,** 864–868.
49. Weber, R., Bridger, J., Benner, A., Weisenberger, D., Ehemann, V., Reifenberger, B. & Lichter, P. (1998) *Cytogenet. Cell Genet.* **83,** 266–269.
50. Kastan, M. B., Onyekwere, O., Sidransky, D., Vogelstein, B. & Craig, R. W. (1991) *Cancer Res.* **51,** 6304–6311.
51. O'Connor, P. M., Jackman, J., Jondle, D., Bhatia, K., Magrath, I. & Kohn, K. W. (1993) *Cancer Res.* **53,** 4776–4780.
52. Kaghad, M., Bonnet, H., Yang, A., Creancier, L., Biscan, J., Valent, A., Minty, A., Chalon, P., Lelias, J., Dumont, M., *et al*. (1997) *Cell* **90,** 809–819.
53. Vaziri, H., West, M., Allsop, R., Davison, T., Wu, Y., Arrowsmith, C., Poirier, G. & Benchimol, S. (1997) *EMBO J.* **16,** 6018–6033.
54. Satoh, M. S. & Lindahl, T. (1992) *Nature (London)* **356,** 356–358.
55. Smulson, M., Istock, N., Ding, R. & Cherney, B. (1994) *Biochemistry* **33,** 6186–6191.